Semiclassical approximation for transmission through open Sinai billiards*

Cai Xiang-Ji(蔡祥吉)[a], Zhang Yan-Hui(张延惠)[a]†, Li Zong-Liang(李宗良)[a], Jiang Guo-Hui(蒋国辉)[a], Yang Qin-Nan(杨秦男)[a], and Xu Xue-You(徐学友)[b]

[a] College of Physics and Electronics, Shandong Normal University, Jinan 250014, China
[b] Information Research Institute, Shandong Academy of Sciences, Jinan 250014, China

(Received 12 April 2012; revised manuscript received 18 July 2012)

We use a semiclassical approximation to study the transport through the weakly open chaotic Sinai quantum billiards which can be considered as the schematic of a Sinai mesoscopic device, with the diffractive scatterings at the lead openings taken into account. The conductance of the ballistic microstructure which displays universal fluctuations due to quantum interference of electrons can be calculated by Landauer formula as a function of the electron Fermi wave number, and the transmission amplitude can be expressed as the sum over all classical paths connecting the entrance and the exit leads. For the Sinai billiards, the path sum leads to an excellent numerical agreement between the peak positions of power spectrum of the transmission amplitude and the corresponding lengths of the classical trajectories, which demonstrates a good agreement between the quantum theory and the semiclassical theory.

Keywords: Sinai billiards, transmission amplitude, classical trajectories, power spectrum

PACS: 05.45.Mt, 73.23.Ad, 03.65.Sq **DOI:** 10.1088/1674-1056/22/2/020501

1. Introduction

In the past 30 years, mesoscopic physics has evolved into a greatly progressing and fascinating field of physics. Mesoscopic systems build a bridge between the microscopic particles which are unobservable and immeasurable by the naked eye, such as atomic electrons, on the one side and the macroscopic objects at the length scale to which Boltzmann transport theory has been applied on the other side.[1,2] Mesoscopic devices, whose dimensions are intermediate between a few nanometers and hundreds of micrometers,[3] exhibit both classical and quantum signatures.[4–6] As the device is being miniaturized day by day, the study on transport in mesoscopic devices has significance and underlying research value.

Two-dimensional quantum billiards have extensively served as model systems in the field of mesoscopic chaotic dynamics.[7] Investigations on quantum billiards have received considerable attention,[8–14] largely due to great progress in the fabrication of submicron semiconductor microstructures which leads to the experimental realization of mesoscopic devices. Semiclassical approximation[15–18] is one of the most beneficial tools to describe and analyze ballistic transport effects in mesoscopic systems. Semiclassical theory, which is used to describe the mesoscopic systems, is a way of handling quantum mechanics problems by a simplified path integral formalism, with a focus on the particle motion of classical mechanics inside the billiards along the trajectories with different numbers of bounces at the boundary, with the purpose of bridging the gap between quantum mechanics and its classical limit.[19–21] Moreover, at a fundamental level, semiclassical approaches allow one to build a link between classical dynamics of the particle motion in the billiards and the quantum leads in a very direct way: each classical trajectory carries an amplitude that reflects its geometric stability and a phase which contains the classical action and accounts for the quantum interference effect.[7,15–18,22,23]

In this paper, in order to study the transport through a 1.0-μm Sinai device of the National Research Council (NRC) of Canada[24] which is depicted in Fig. 1(a), we use a semiclassical approximation to calculate the transmission power spectrum of the open Sinai billiards, and in Fig. 1(b) between the two leads of the billiards we investigate the correspondence between the peak positions of the transmission power spectra and the corresponding lengths of the classical trajectories for short paths. In the semiclassical approximation, the motion of the particle in the leads is well described by quantum mechanics, whereas that inside the billiards is depicted by semiclassical theory. Due to the fact that the width of each of the leads is comparable to the de Broglie wavelength, the diffraction effect at the lead opening within the framework of the Fraunhofer diffraction[19] should be taken into account.

The rest of this paper is organized as follows. In Section 2 we introduce the semiclassical approximation including the diffraction effect at the lead openings within the framework of the Fraunhofer diffraction down to the last detail. Numerical results and discussion on the comparison between the length of the classical trajectory and the corresponding peak

*Project supported by the National Natural Science Foundation of China (Grant Nos. 10804064 and 10774093).
†Corresponding author. E-mail: yhzhang@sdnu.edu.cn
© 2013 Chinese Physical Society and IOP Publishing Ltd

position, and the power spectra of the reflection amplitude are given in Section 3. The conclusions drawn from the present study and the future applications are presented in the last section.

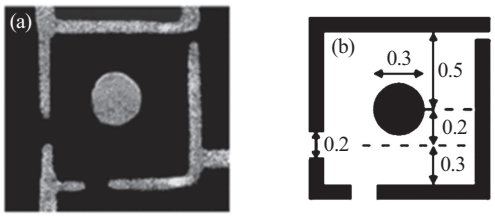


Fig. 1. (a) Scanning electron micrograph of the NRC Sinai device, and (b) schematic plot of the NRC Sinai device. All dimensions are in μm.

2. Semiclassical approximation

As depicted in Fig. 2, the billiards is defined by an open square of side length L with two perpendicular leads of equal width d determining the outer boundary and a circle with radius R in the centre defining the inner boundary. The electron enters into lead i at an angle of incidence in an interval $(-\pi/2, \pi/2)$. There is no external potential inside the region between the inner and the outer boundary, and the electron moves freely within the billiards, along a straight line, until it encounters the hard-wall boundary where it reflects specularly.

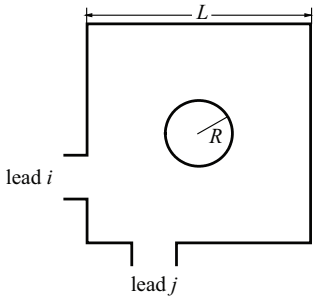


Fig. 2. Sketch of the Sinai billiards with two perpendicular leads of equal width d.

The conductance g for ballistic transport as a function of wave number k through the two-terminal open billiards system (as depicted in Fig. 2) is given by Landauer formula[25]

$$g(k) = \frac{2e^2}{h} T(k) = \frac{2e^2}{h} \left(\sum_{m=1}^{M} \sum_{n=1}^{M} |T_{n,m}(k)|^2 \right), \qquad (1)$$

where $T(k)$ is the total transmission probability, and $T_{n,m}(k)$ is the transmission amplitude from transverse mode m in the entrance lead i to mode n in the exit lead j. M is the number of total open modes in the leads of equal width d, and each mode corresponds to a quantized eigenstate in the lead perpendicular to the flux direction. Each of the two leads has $m = 1, \ldots, M$ open modes in total.

The corresponding m-th transverse wave function in lead i of width d with infinitely high potential walls is

$$\phi_{i,m}(y_i) = \sqrt{\frac{2}{d}} \sin\left[\frac{m\pi}{d} \left(y_i + \frac{d}{2} \right) \right]. \qquad (2)$$

Due to the quantization of the transverse momentum in the lead, the electron enters into and exits from the billiards at the discrete quantized angle

$$\theta_n = \pm \arcsin\left(\frac{n\pi}{dk} \right). \qquad (3)$$

Here and in the following, atomic units are used with $\hbar = |e| = m_e = 1$. For an electron at the Fermi energy $E = k^2/2$, which is approaching to the billiards, the wave functions of the entrance lead i and the exit lead j are given by

$$\begin{aligned} \psi_m^1(y_i) &= \sqrt{\frac{1}{k_{x_i,m}}} \varphi_{i,n}(y_i) \, \mathrm{e}^{\mathrm{i} k_{x_i,m} x_i} \\ &\quad + \sum_{n=1}^{M} r_{n,m} \sqrt{\frac{1}{k_{x_i,n}}} \varphi_{i,n}(y_i') \, \mathrm{e}^{-\mathrm{i} k_{x_i',n} x_i'} \quad \text{for } i = j, \qquad (4) \\ \psi_m^2(y_j) &= \sum_{n=1}^{M} t_{n,m} \sqrt{\frac{1}{k_{x_j,n}}} \phi_{j,n}(y_j) \, \mathrm{e}^{\mathrm{i} k_{x_j,n} x_j} \quad \text{for } i \neq j. \qquad (5) \end{aligned}$$

The elements $S_{n,m}^{(j,i)}(k)$ of the S-matrix delineate the scattering for incidence from transverse mode m in the entrance lead i to mode n in lead j. For a two-terminal open billiards, the transmission amplitude from transverse mode m in the entrance lead i to mode n in the exit lead j is denoted as $T_{n,m}(k) = S_{n,m}^{(j,i)}(k)$ for $i \neq j$, while the reflection amplitude from transverse mode m in the entrance lead i back into mode n in lead i is denoted as $R_{n,m}(k) = S_{n,m}^{(j,i)}(k)$ for $i = j$.

The transmission amplitude $t_{n,m}(k)$ from the m-th incoming mode in the entrance lead i to the n-th outgoing mode in the exit lead j is customarily expressed as the projection of the Green's function on the transverse wave functions $\phi_m(y_i)$ and $\phi_n(y_j)$ of the incoming and outgoing modes

$$\begin{aligned} T_{n,m}(k) &= -\mathrm{i} \sqrt{k_{x_j,n} k_{x_i,m}} \int \mathrm{d}y_j \int \mathrm{d}y_i \phi_n^*(y_j) \\ &\quad \times G(y_j, y_i, k) \, \phi_m(y_i), \qquad (6) \end{aligned}$$

where $k_{x_i,m} = \sqrt{k^2 - |m\pi/d|^2}$ $\left(k_{x_j,n} = \sqrt{k^2 - |n\pi/d|^2} \right)$ is the longitudinal component of the wave number of the incoming (outgoing) wave function and y_i (y_j) is the longitudinal coordinate parallel to lead i (lead j). The prefactor $\sqrt{k_{x_j,n} k_{x_i,m}}$ is due to flux normalization.

Replace $G(y_j, y_i, k)$ in Eq. (6) by the semiclassical Green's function of a two-dimensional free particle in terms of classical path to describe the constant energy transfer from y_i in the opening of the entrance lead i with y_j in the opening of the exit lead j, which is

$$G^{\mathrm{SC}}(y_j, y_i, k) = \sum_{\alpha: y_i \to y_j} G_\alpha^{\mathrm{SC}}$$

$$= \sum_{\alpha:y_i\to y_j} \frac{\left|D_\alpha(y_j,y_i,k)\right|^{1/2}}{(2\pi i)^{1/2}} \times \exp\left[i\left(S_\alpha(y_j,y_i,k)-\frac{\pi}{2}\mu_\alpha\right)\right]. \quad (7)$$

In Eq. (7), the summation extends over all possible classical paths α connecting y_i in the entrance lead opening with y_j in the exit lead opening; $S_\alpha(y_j,y_i,k)=kL_\alpha(y_j,y_i)$ is the action of path α, with L_α being the length of the path that connects the centre of the entrance with the exit lead openings; $D_\alpha(y_j,y_i,k)$ is the classical deflection factor (weighting factor) which is a measure for the divergence of nearby trajectories to describe the stability of the path; μ_α denotes the Maslov index of the path α. When a trajectory is folded at a time, the Maslov index increases by 1 and the wave undergoes a phase loss of $\pi/2$.

The transmission power spectrum is defined as the Fourier transformation of the transmission amplitude $t_{n,m}(k)$

$$T_{n,m}(L)=\int \mathrm{e}^{-\mathrm{i}kL}T_{n,m}(k)\,\mathrm{d}k. \quad (8)$$

Considering the diffractive scattering effect at the lead openings, the diffraction coefficient of the transmission amplitude from the m-th incoming mode in the entrance lead with angle of incidence θ_α corresponding to one classical path α is given by the Fraunhofer diffraction approximation as[17]

$$t_m(\theta_\alpha,k) = \sqrt{\frac{2\cos\theta_\alpha}{kd}}\left\{\frac{\sin\left[\left(k\sin\theta_\alpha+\frac{m\pi}{d}\right)\frac{d}{2}\right]}{\sin\theta_\alpha+\frac{m\pi}{kd}} + \frac{\sin\left[\left(k\sin\theta_\alpha-\frac{m\pi}{d}\right)\frac{d}{2}\right]}{\sin\theta_\alpha-\frac{m\pi}{kd}}\right\}. \quad (9)$$

Then the transmission amplitude $t_{n,m}(k)$ is written as

$$t_{n,m}(k)=\sum_\alpha t_n(\theta'_\alpha,k)G^{\mathrm{SC}}(\theta'_\alpha,\theta_\alpha,k)t_m(\theta_\alpha,k), \quad (10)$$

where θ_α is the incident angle into the billiards, θ'_α is the emergent angle out of the billiards for path α, and $G^{\mathrm{SC}}(\theta'_\alpha,\theta_\alpha,k)$ is the Green's function connecting the incident angle θ_α with the emergent angle θ'_α of the path α.

3. Numerical results and discussion

In this section, we present the numerical results for the transmission power spectrum within the framework of our semiclassical approximation considering the diffractive scattering effect at the lead openings, the results calculated by the standard semiclassical approximation, and the comparison between the lengths of the classical trajectories and the corresponding peak positions, and the power spectra of the reflection amplitude.

First, we list the parts of the classical trajectories of the free particle inside the Sinai billiards (as depicted in Fig. 2) with different numbers of bounces at the boundary according to classical dynamics. The particle enters into the billiards along trajectories with different numbers of bounces at the boundary from the centre of the left lead i and ejects from the centre of the perpendicular lead j.

In the following, we show the power spectra of the transmission amplitude t_{11} for the first mode, calculated for the finite number of trajectories with lengths shorter than 5.0 in Fig. 4.

Each peak in the power spectrum corresponds to one or more classical trajectories of the same length between the entrance and the exit leads. The position of the peak is the length of the corresponding trajectory and the height of the peak is calculated accurately by Eq. (8).

In Table 1, we present the comparison between the peak positions of the transmission power spectra, obtained from the semiclassical approximation, and the corresponding lengths of the classical trajectories with several bounce numbers according to classical dynamics.

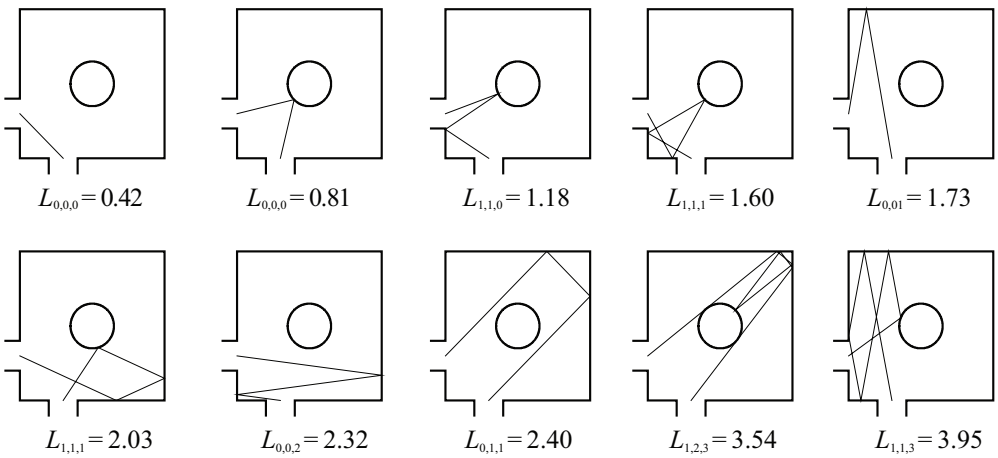


Fig. 3. Parts of the classical trajectories in the Sinai billiards.

Table 1. Comparisons between the lengths of the classical trajectories and the corresponding peak positions.

Trajectory shape	$L_{0,0,0}$	$L_{1,0,0}$	$L_{1,1,0}$	$L_{1,0,1}$	$L_{1,1,1}$	$L_{0,0,1}$	$L_{0,1,0}$	$L_{1,1,0}$	$L_{1,0,1}$
Peak position	0.4	0.9	1.2	1.2	1.5	1.7	1.7	1.9	1.9
Trajectory length	0.42	0.81	1.18	1.18	1.60	1.73	1.73	1.89	1.89
Trajectory shape	$L_{1,1,1}$	$L_{1,1,1}$	$L_{0,0,2}$	$L_{0,2,0}$	$L_{0,1,1}$	$L_{1,1,2}$	$L_{1,2,1}$	$L_{1,2,1}$	$L_{1,1,2}$
Peak position	2.0	2.0	2.2	2.2	2.3	2.5	2.5	2.8	2.8
Trajectory length	2.03	2.03	2.32	2.32	2.40	2.51	2.51	2.97	2.97
Trajectory shape	$L_{1,2,2}$	$L_{0,0,3}$	$L_{0,3,0}$	$L_{1,3,1}$	$L_{1,1,3}$	$L_{0,0,4}$	$L_{0,4,0}$	$L_{2,3,3}$	$L_{2,3,3}$
Peak position	3.4	3.6	3.6	3.8	3.8	4.3	4.3	4.6	4.6
Trajectory length	3.54	3.71	3.71	3.95	3.95	4.31	4.31	4.60	4.60

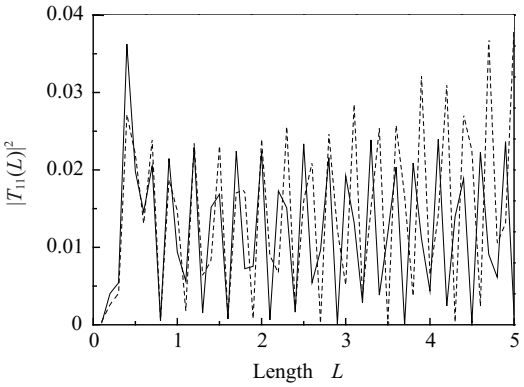


Fig. 4. Power spectra of the transmission amplitude for T_{11}, calculated by our semiclassical approximation (solid curve) and by the standard semiclassical approximation (dashed curve), in a finite interval of k, $1 \leq k \leq 3$ in units of π/d.

Examination of the curve as depicted in Fig. 4 and the comparison in Table 1, display that the peak value is generally too small due to the fact that we use the finite number of trajectories with the lengths $L \leq 5.0$ in the semiclassical calculation. By comparison, we find that one or more classical trajectories of the same lengths with different bounce numbers correspond to the same peak, while those of different lengths with the same bounce number correspond to different peaks. The largest peak, at $L \sim 0.4$, corresponds to a classical trajectory that the electron moves directly along a straight line from the centre of the entrance lead opening to that of the exit lead opening without any bounce with the hard-wall boundary. However, we find that there is no classical trajectory corresponding to the second peak, at $L \sim 0.6$. The reason is that the width d of the quantum lead is 0.2, and the length of the trajectory is permitted to float in the region from 0 to 0.2.

Figure 5 displays the power spectrum of the reflection amplitude R_{11} for the first mode.

Theoretically, the reflection amplitude should contain prominent contributions from a series of "ghost paths",[15] which are nonclassical paths reflected back into the billiards but not exiting from the lead opening due to the diffraction effects. For instance, there should be a peak at $L \sim 0.4$, caused by the direct ghost path where the electron moves directly along a straight line from the entrance lead opening to the exit lead opening and back. No peak appears at the ghost path in our calculation, for which the reason is that we calculate the internal propagation within the billiards in terms of the semiclassical Green's function G^{SC}.

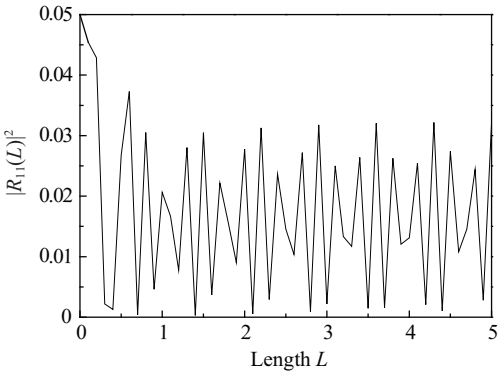


Fig. 5. Power spectrum of reflection amplitude R_{11}, calculated by our semiclassical approximation in a finite interval of k, $1 \leq k \leq 3$ in units of π/d.

4. Concluding remarks and outlook

We use a semiclassical approximation to study the transport through the weakly open chaotic Sinai billiards, and the diffractive scatterings at the lead openings are considered. With the semiclassical approximation, we analyze the transmission power spectrum and find an excellent numerical agreement between the power spectra of the transmission amplitudes and the corresponding lengths of the classical trajectories for short paths. However, the secondary effect of the increasing number of bounces and the destructive interference between the adjacent trajectories for long paths cause path shadowing of some classical trajectories and some peaks corresponding to the classical trajectories to be reduced, which makes the semiclassical approximation inapplicable for the long path case. All the results we obtained in the semiclassical approximation show a close correspondence between the quantum and the classical dynamical characteristics for the transport through the weakly open chaotic Sinai billiards. Combining our previous study[26,27] on the transport through the weakly open integrable billiards, we find a good agreement between the peak positions of the transmission power spectra and the corresponding lengths of the classical trajectories

for short paths in both the integrable and the chaotic billiards, which demonstrates an excellent correspondence between the quantum theory and the semiclassical theory. However, in our numerical calculation, we calculate the power spectrum of the transmission amplitude for the first mode by using the finite number of short paths. Furthermore, the contributions from longer paths and higher modes should be taken into account.

References

[1] Sohn L L 1998 *Nature* **394** 131
[2] Ferry D K, Goodnick S M and Bird J 2009 *Transport in Nanostructures* 2nd edn. (Cambridge: Cambridge University Press) p. 2
[3] Datto S 1995 *Electronic Transport in Mesoscopic Systems* (Cambridge: Cambridge University Press) p. 1
[4] Richter K 2000 *Semiclassical Theory of Mesoscopic Quantum Systems* (New York: Springer-Verlag) p. 1
[5] Heinzel T 2007 *Mesoscopic Electronics in Solid State Nanostructures* 2nd edn. (KGaA: WILEY-VCH Verlag GmbH & Co.) p. 2
[6] Ihn T 2010 *Semiconductor Nanostructures Quantum States and Electronic Transport* (Oxford: Oxford University Press) p. 95
[7] Gutzwiller M C 1990 *Chaos in Classical and Quantum Mechanics* (New York: Springer-Verlag) p. 3
[8] Du M L and Delos J B 1987 *Phys. Rev. Lett.* **58** 1731
[9] Du M L and Delos J B 1988 *Phys. Rev.* A **38** 1896
[10] Lu J and Du M L 2004 *Acta Phys. Sin.* **53** 2450 (in Chinese)
[11] Xu X Y, Zhang Y H, Huang F Z, Lin S L and Du M L 2005 *Acta Phys. Sin.* **54** 4538 (in Chinese)
[12] Zhang Y H, Zhang L Q, Xu X Y, Ge M H, Lin S L and Du M L 2006 *Chin. Phys.* **15** 502
[13] Zhang Y H, Zhang J Q, Xu X Y and Lin S L 2009 *Chin. Phys.* B **18** 35
[14] Zhang J Q, Zhang Y H, Zhou H, Jia Z M and Lin S L 2009 *Acta Phys. Sin.* **58** 5965 (in Chinese)
[15] Schwieters C D, Alford J A and Delos J B 1996 *Phys. Rev.* B **54** 10652
[16] Wirtz L, Tang J Z and Burgdörfer J 1997 *Phys. Rev.* B **56** 7589
[17] Wirtz L, Stampfer C, Rotter S and Burgdörfer J 2003 *Phys. Rev.* E **67** 016206
[18] Stampfer C, Rotter S and Burgdörfer J 2005 *Phys. Rev.* E **72** 036223
[19] Brack M and Bhaduri R K 1997 *Semiclassical Physics* (Reading Mass: Addison-Wesley Publishing Company) p. 1
[20] Nazmitdinov R G, Pichugin K N, Rotter I and Šeba P 2002 *Phys. Rev.* B **66** 085322
[21] Sohn L L, Kouwenhoven L P and Schön G 1997 *Mesoscopic Electron Transport* (Boston: Kluwer Academic Publishers) p. 106
[22] Berry M V and Mount K E 1972 *Rep. Prog. Phys.* **35** 315
[23] Feynman R P and Hibbs A R 1965 *Quantum Mechanics and Path Integrals* (New York: MacGraw-Hill) p. 31
[24] Berry M J, Baskey J H, Westervelt R M and Gossard A C 1994 *Phys. Rev.* B **50** 8857
[25] Landauer R 1957 *IBM J. Res. Dev.* **1** 223
[26] Xu X Y, Wang S B, Jia Z M and Lin S L 2007 *J. At. Mol. Phys.* **5** 999 (in Chinese)
[27] Xu X Y, Zhang Y H, Li H Y, Gao S and Lin S L 2008 *Chin. Phys. Lett.* **25** 1549